Author(s): Miettunen, Kati & Vapaavuori, Jaana & Tiihonen, Armi & Poskela, Aapo & Lahtinen, Panu & Halme, Janne & Lund, Peter

Title: Nanocellulose aerogel membranes for optimal electrolyte filling in dye solar cells

Year: 2014

Version: Post print

Please cite the original version:

Miettunen, Kati & Vapaavuori, Jaana & Tiihonen, Armi & Poskela, Aapo & Lahtinen, Panu & Halme, Janne & Lund, Peter. 2014. Nanocellulose aerogel membranes for optimal electrolyte filling in dye solar cells. Nano Energy. Volume 8. 95-102. ISSN 2211-2855 (printed). DOI: 10.1016/j.nanoen.2014.05.013.

Nanocellulose aerogel membranes for optimal electrolyte filling in dye solar cells

Kati Miettunen*[,a], Jaana Vapaavuori [b,c], Armi Tiihonen [a], Aapo Poskela [a], Panu Lahtinen [d], Janne Halme [a], Peter Lund [a]

[a] Aalto University, New Energy Technologies Group, Department of Applied Physics, P.O. BOX 15100, FIN-00076 AALTO, Finland
[b] Aalto University, Optics and Photonics Group, Department of Applied Physics, P.O. BOX 13500, FIN-00076 AALTO, Finland
[c] University of Montreal, Department of Chemistry, C.P. 6128, Succursale Centre-Ville, Montreal (QC), H3C 3J7 Canada
[d] VTT Technical Research Centre of Finland, P. O. Box 1000, FI-02150 Espoo, Finland

Abstract

A new method for depositing the electrolyte in dye solar cells (DSCs) is introduced: a nanocellulose hydrogel membrane is screen printed on the counter electrode and further freeze-dried to form a highly porous nanocellulose aerogel, which acts as an absorbing sponge for the liquid electrolyte. When the nanoporous dye-sensitized TiO_2 photoelectrode film is pressed against the wetted aerogel, it becomes filled with the electrolyte. The electrolyte flows inside the TiO_2 film only about ten micrometers (i.e. the TiO_2 film thickness) whereas in the conventional filling method, where the electrolyte is pumped through the cell, it flows about 1,000-times longer distance, which is known to cause uneven distribution of the electrolyte components due to a molecular filtering effect. Furthermore, with the new method there is no need for electrolyte filling holes which simplifies significantly the sealing of the cells and eliminates one common pathway for leakage. Photovoltaic analysis showed that addition of the nanocellulose aerogel membrane did not have a statistically significant effect on cell efficiency, diffusion in the electrolyte or charge transfer at the counter electrode. There was, however, a clear difference in the short circuit current density and open circuit voltage between the cells filled with the aerogel method and in the reference cells filled with the conventional method, which appeared to be caused by the differences in the electrolyte filling instead of the nanocellulose itself. Moreover, accelerated aging tests at 1 Sun 40 °C for 1000 h showed that the nanocellulose cells were as stable as the conventional DSCs. The nanocellulose aerogel membranes thus appear inert both with respect to performance and stability of the cells, which is an important criterion for any electrolyte solidifying filler material.

Keywords: nanocellulose; semi-solid electrolyte; gel electrolyte; dye-sensitized solar cell; spatial distribution

* Corresponding author: Telephone: +358 50 3441729.
E-mail address: kati.miettunen@aalto.fi.

1. Introduction

Dye sensitized solar cells, also known as dye solar cells (DSC), are based on cheap materials and easy preparation methods. Scaling up towards mass production roll-to-roll processes may offer an additional way to keep the manufacturing costs low [1,2]. Printing a dye solar cell involves several steps, but so far finding a printable electrolyte has been one of the bottlenecks [2]. Normally, the electrolyte is in liquid form which causes difficulties in the assembly and handling of the cell. When employing conventional filling methods, the electrolyte is pumped through the cell which is inconvenient for mass production purposes. Also, the porous dyed TiO_2 layer acts as a filter adsorbing some of the electrolyte additives leading to an uneven distribution of the electrolyte components in the cell. Hence, significant spatial variations in the performance may result [3-6]. The efficiency losses due to this spatial effect have been as high as 35% [4]. The effects can be reduced to some extent by changing e.g. the electrolyte composition [4-6]. Optimally, the electrolyte filling method should intrinsically result in an even spatial distribution.

For a printed electrolyte one would prefer a low cost and a high performance. The practical issue is to form an electrolyte which would not spill under the edge sealant, but would still pass easily through the porous TiO_2 layer. Semi-solid electrolytes are an attractive, although to date largely unexplored solution to these problems: Mixing the normal liquid electrolyte either with polymers and/or nanoparticles have been proposed. Among those there are no recipes for printed electrolytes for DSCs. Another way to make a semi-solid electrolyte is to fill a porous polymer membrane with a liquid electrolyte [7,8]. To avoid any interference between such a membrane and the operation of the cell, the membrane should be thin to avoid a thick cell structure, and highly porous to enable a high charge transfer in the cell. In practice, fulfilling both requirements simultaneously and having a membrane that can be handled without breaking is problematic [7,8].

Here we propose to use a nanocellulose aerogel membrane, which can be prepared by freeze-drying the nanocellulose hydrogel printed directly on the counter electrode. The nanocellulose aerogel serves as an absorbent for the electrolyte withholding it from spreading on the substrate and since the aerogel is supported by the counter electrode, the membrane can be made both highly porous and very thin. The nano-cellulose “sponge” is wetted with the electrolyte prior to the assembly of the cell. When the cell is encapsulated, the electrolyte sponge wets also the photoelectrode side of the cell. In this way the electrolyte comes into contact with the dyed TiO_2 film spatially, and it is not pushed laterally through the cell, which is important to achieve an even distribution of electrolyte components (Figure 1). Additionally, holes for filling the electrolyte are unnecessary, improving the reliability of the encapsulation. Nanocellulose is an interesting material for many practical applications, since it has multiple benefits; it derives from economic, abundant and renewable resources. In addition, being a non-toxic and sustainable biopolymer, it can be regarded environmentally-friendly. Relatively similar absorbing nanocellulose sponges, that herein are used to support the solar cell electrolyte, have been suggested as a solution to other environmental problems, such as cleaning the oil spills in marine environments [9].

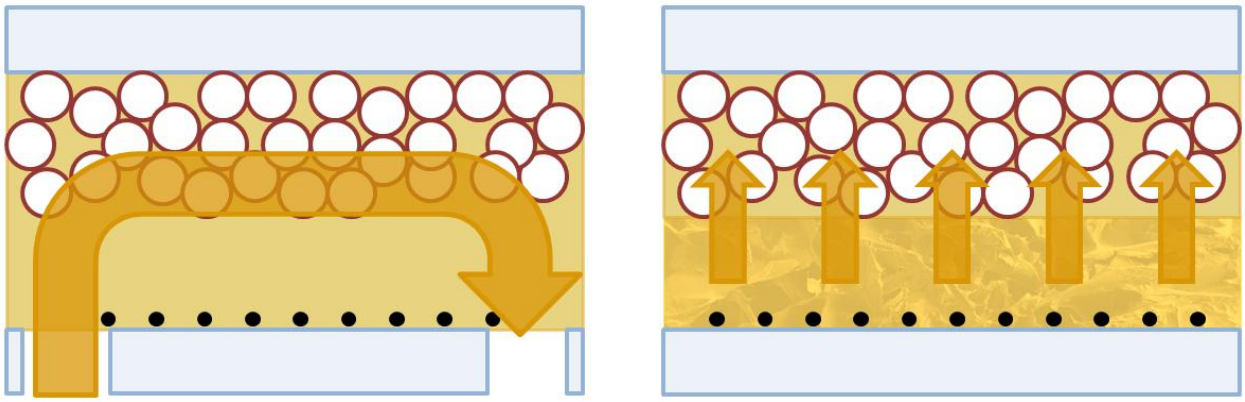

Figure 1. Schematics of the electrolyte filling process in the conventional filling through the filling holes (left) and the filling using the nanocellulose aerogel (right). The arrows indicate direction of the electrolyte flow.

2. Material and methods

2.1 Cell preparation

Fluorine-doped tin oxide (FTO) glass (TEC-15, Pilkington) was used as substrates for all of the prepared DSCs. By using glass substrates, we can avoid any questions related to the stability of the substrate which simplifies the stability analysis. The catalyst for the counter electrode was made by spreading 4 µl of 5 mM H_2PtCl_6 in 2-propanol on a clean substrate and then it was heated at 390 ºC for 15 min. After the Pt catalyst layer was prepared, the nanocellulose hydrogel was screen printed on top of the counter electrodes by a screen printer (AT-60PD, ATMA) equipped with a mesh (NBC, 43-080 22.5º). Cellulose nanofibres were made of never-dried bleached birch kraft pulp and pre-treated as described elsewhere [10,11]. The gel was prepared by feeding the modified fibre suspension into a Microfluidizer M-7115-30. The fluidizer was equipped with a pair of ceramic (500 µm) and diamond (200 µm) chambers. The slurry had dry content of 1.0 wt. % and it passed once through the chambers at the operating pressure of 1500 bar. After the printing, the layers were instantly frozen in liquid nitrogen, followed by vacuum freeze-drying to give nanocellulose aerogels with over 98% porosity, as reported previously [12]. The resulting membranes were on average about 10 µm thick. Since the nanocellulose hydrogel was not customized for screen printing the mesh left its mark as height variation in the film. Since the nanocellulose has only the purpose of restraining the electrolyte, the variation in height did not affect this main feature as Figure 2 indicates. We have also tested that this aerogel membrane preparation method works with flexible ITO coated PET plastic substrates.

The photoelectrodes were made on FTO glass to simplify the analysis. A $TiCl_4$ treatment was given to the photoelectrode substrate before adding the TiO_2 layers: the substrates were placed in a solution of titanium (IV) chloride tetrahydrofuran complex (1 wt-%) in distilled water and then heated in 70 ºC for 30 min [13]. Three layers of TiO_2 were screen printed: the first two using a paste with small TiO_2 particles (Dyesol, 18NR-T) and the last layer using TiO_2 paste with large light scattering particles (Dyesol, WER2-0). After printing, the photoelectrodes were sintered in

an oven at 450 ºC for 30 minutes. The resulting porous TiO_2 layers had the total thickness of about 13-14 µm and an area of 40 mm^2. When the photoelectrodes had cooled down, they were given another $TiCl_4$ treatment as described above and then sintered again at 450 ºC. The TiO_2 layers were dyed in 0.3 mM cis-Bis(isothiocyanato)(2,2′-bipyridyl-4,4′-dicarboxylato)(4,4′-di-nonyl-2′-bipyridyl) ruthenium(II) (Z907, Dyesol) in 1:1 acetonitrile/tert-butyl alcohol solution.

Before the electrodes were put together, the porous nanocellulose film at the counter electrode was wetted with electrolyte (HSE-EL electrolyte, Dyesol). The electrodes were attached together with a Surlyn 1702 frame foil which melted at 120 ºC. In the reference glass cells, the electrolyte was filled into the cell through the filling holes and those were encapsulated with another Surlyn foil and a thin cover glass. Copper tapes were used as external connectors and silver paint (Electrolube) was spread to the copper tape / substrate interface to improve conductivity. Finally, epoxy was applied over the interface area to improve the durability of the contact.

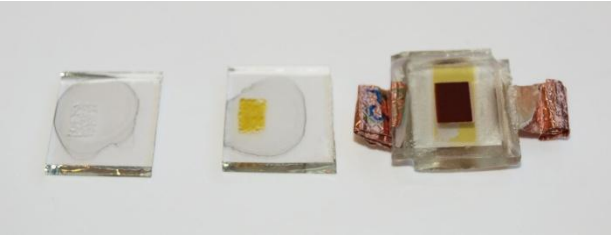

Figure 2. A picture of the printed nanocellulose membrane (left), the membrane wetted with electrolyte (center), and a complete dye solar cell made using the membrane (right). Note that due to a non-optimized thickness and size of the membrane in this case, the electrolyte spreads also laterally as the cell is sealed. The ideal situation where the lateral flow is minimized (Figure 1), can be approached by adjusting the dimensions of the aerogel membrane.

2.2 Measurements

Photovoltaic measurements for the solar cells were conducted using a solar simulator with halogen lamps (Philips type 13117). The simulator generated an output equivalent to solar output in AM1.5G, so called 1 Sun. Black masks, that had holes that were 1 mm wider than the active area of the cell, were used to reduce the edge effects as advised in the literature [14].

Electrochemical impedance spectroscopy (EIS) measurements were performed with Zahner Zennium. The cells were measured at the open-circuit conditions in the solar simulator at the same time with the photovoltaic measurements. The cells were measured also in dark over the voltage range from 0.0 V to 0.7 V with 0.1 V intervals. In both cases the set frequency range was 100 mHz - 100 KHz and the amplitude 10 mV. The equivalent circuit fitting was done to the EIS spectra using ZView2 (Scribner Associates, Inc.) and the equivalent circuits used here are presented in our previous work [17].

Incident photon to collected electron (IPCE) measurements were performed with Measurement system QEX7 (PV Measurements, Inc.). The studied wavelength range was 300-1000 nm in 2 nm intervals and the measurements were executed in DC mode.

A stability test (1000 h, approximately 1 Sun, 40 ºC) was done to the cells. The aging was carried out using similar lamps as in the photovoltaic measurements. A UV filter (cut-off 400 nm, SFC-10 clear, Asmetec) was employed to block the long term effects of UV light. In comparison with the solar simulator measurements, in these measurements no masks were used on top of the cells and longer wiring was required for the measurement setup which resulted in slightly increased resistance. During the aging, the photovoltaic performance of the cells was recorded with a Biologic SP-150 using a Agilent 34980A as a multiplexer.

The scanning electron microscope (SEM) images were taken with Zeiss Σigma VP system using 2 keV electron energy.

3. Results and discussion

3.1 Structure of the nanocellulose layer

Figure 3 shows the scanning electron microscopy image of the used nanocellulose aerogel film. During the freezing of the hydrogel, the ice crystals press the nanocellulose fibers to form thin sheet-like structure [15]. This particular structure might play a key role in the ability of the membrane to hold the electrolyte in its place as shown in Figure 2, which before this technique was seen as one of the biggest challenges. An interesting question is how the membrane affects charge transfer in the electrolyte. The porosity of the sheet structure is very high and the area of the air-filled sections that are defined by the nanocellulose are quite large, in the order of 20 µm (Figure 3). Based on the SEM images alone it is difficult to estimate the effects of the structure to diffusion. Another thing that is important for the operation of the dye solar cell is that the catalyst layer is not blocked by the membrane. The effects of the membrane on these charge transfer reactions are evaluated in Sections 3.2 and in particular 3.4.

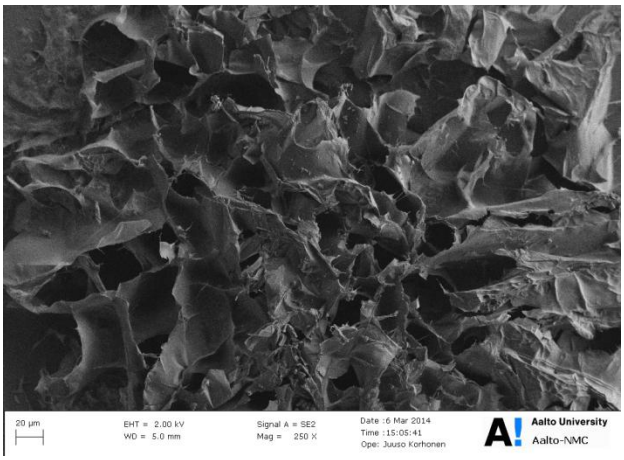

Figure 3. SEM image of the nanocellulose membrane on the counter electrode.

3.2 Photovoltaic performance

The cells with the nanocellulose membrane reached as high efficiency as the reference cells with conventionally filled liquid electrolyte (Table 1). There are, however, differences in the other characteristics of the cell performance: nanocellulose cells have about 20 % higher short circuit current density I_{SC} but lower open circuit voltage V_{OC} and *FF*. The two major differences in the nanocellulose cells and the reference cells were the presence of the nanocellulose and the preparation of the cell, in particular filling of the electrolyte.

When a new material is added to the cell, it is imperative to investigate, if it creates adverse effects. Here the overall efficiency did not change, but there was a “trade-off” difference in the other photovoltaic parameters. If the nanocellulose layer could improve optics and thus increase the current, a trade-off could be possible. However, any optical effect that could improve the photocurrent production can be omitted as the photoelectrodes had a completely opaque back reflector layer. This means that whatever was behind it, such as the nanocellulose layer, should not affect the light absorption in the cell. Hence it is difficult to form a hypothesis how the presence of nanocellulose as such could cause this kind of effect.

In contrast, the way how the electrolyte comes in touch with the photoelectrode has been shown to have the observed effect on the performance characteristics [3-6]. In the reference cells, the electrolyte is pushed laterally through the dyed TiO_2 film (length 8 mm). In the nanocellulose cells, the electrolyte comes horizontally into the dyed TiO_2 film (length about 13-14 µm). In other words, there is almost three orders of magnitude difference in how far the electrolyte needs to travel in the TiO_2 film. If the TiO_2 film, acting as a filter, is longer, there can be more spatial differences but it can also “filter” in total a larger part of the additives in the electrolyte. Hence, in the conventionally filled cells, there would be more additives adsorbed on the surface of the dyed TiO_2. The electrolytes in dye solar cells commonly contain an agent, typically 4-tert-butylpyridine (4-tBP) or N-methyl-benzimidazole (NMBI), that increases the cell voltage, but reduces the current by shifting the level of TiO_2 conduction band [16-18]. Here we applied a commercial electrolyte so unfortunately the used voltage increasing agent is unknown to us. Based on previous studies, it is known that the effects of different voltage increasing agents are quite similar [3-5] and the commercial electrolyte used here is known to have similar spatial

performance issues as the ones with known compositions [4]. It is seems very likely that here the reference cells have a higher voltage as significantly larger amount of the voltage increasing agent has been adsorbed in the dyed TiO_2 film in the electrolyte filling. These additives shift the conduction band of the TiO_2 higher to get the higher voltage, but at the same time it makes electron injection more difficult which often reduces the photocurrent. The data shown in Table 1 indicates these kinds of differences between the nanocellulose and reference cells. In the literature, segmented cell with 5 mm segment length had significant differences in the performance of consecutive segments [5,6]. If the effects here are caused by the filling as suspected, they indicate how large difference the filling method can cause even in small laboratory sized device (i.e. active area below 1 cm^2).

To investigate the reliability of our hypothesis of the electrolyte filling causing the effects, we managed to prepare and seal one cell similar to the nanocellulose cells but without the nanocellulose film (i.e. having just droplets of electrolyte on the counter electrode). This was difficult as there was nothing to hold the electrolyte in its place and prevent it from spilling out as the cell was sealed. Hence there is only one such cell to compare to. But interestingly this cell gave the same kind of performance (less than 5 % difference in each parameter listed in Table 1) as the best nanocellulose cell. This suggests that the difference was indeed in the preparation method of nanocellulose cells rather than the nanocellulose itself as our above-mentioned deduction also implies.

Above, we have discussed how the filling method could result in a difference in V_{OC} and I_{SC}, but not yet how it could affect *FF*. Additionally, nanocellulose could reduce *FF* by slowing down the diffusion in the electrolyte and/or charge transfer at the counter electrode as it could block some of the catalyst. Hence careful investigation of factors affecting *FF* is needed. When there are difference in I_{SC} and V_{OC}, it often reflects also on *FF* without there being any other changes in the cell. Here the difference between I_{SC} values is much greater than in V_{OC} (Table 1) which would lead to difference in *FF*. If I_{SC} gets larger and the resistances in the cell remain constant, it results in a lower *FF*. Hence comparison of *FF* values in such a case is not the most reliable option to investigate differences in charge transfer. In contrast, it is better to examine the slope of the photovoltaic curve at OC condition to gain information about the differences in the so-called series connected resistances in the cell [19] and this parameter is marked here as R_{cell}. Table 1 shows that the cells did have similar R_{cell} values which suggests that the series connected resistances have not been affected by the addition of nanocellulose. Therefore, the change in *FF* appears to be predominantly due to the shifts in I_{SC} and V_{OC}, and there does not appear to be related to any significant changes in the charge transfer processes in the cell. However, R_{cell} is composed of several different factors and, although the total value was the same in both types of cells (Table 1), it is worth investigating possible differences in the individual components. This is done in Section 3.4 with impedance spectroscopy.

Table 1. Average performance characteristics and related standard deviation in the initial measurements.

	number of cells	I_{SC} [mA/cm^2]	V_{OC} [mV]	*FF* [%]	η [%]	R_{cell} [Ω]
nanocellulose cells	3	11.7 ± 1.4	698 ± 9	57 ± 3	4.7 ± 0.8	37 ± 7
reference cells	4	9.7 ± 0.7	752 ± 7	66 ± 2	4.8 ± 0.2	38 ± 3

3.3 Analysis of the differences in photocurrent

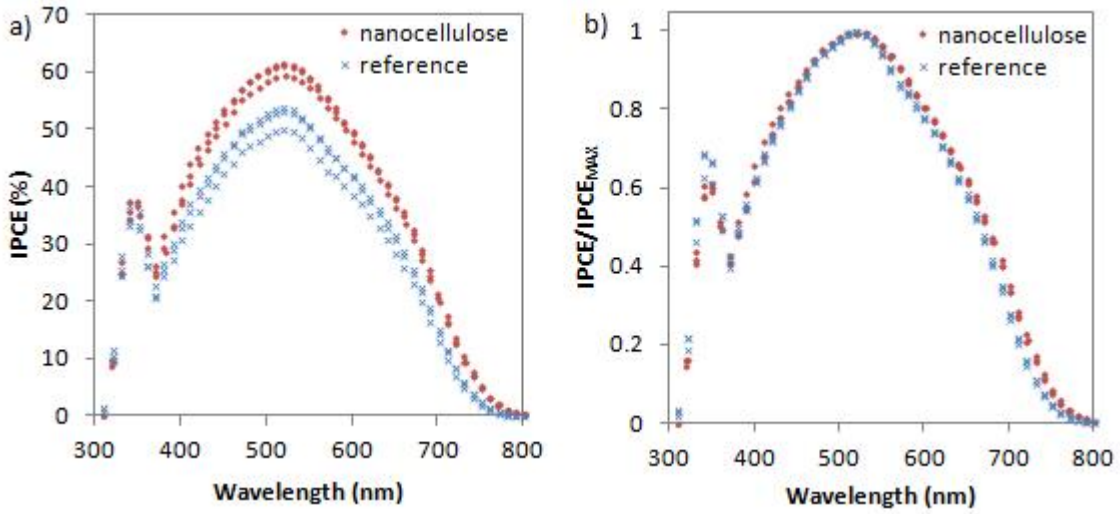

Figure 4. a) The measured IPCE and b) normalized initial IPCE data of nanocellulose cells and the reference cells. Data of three similar cells of each type are shown to represent the repeatability of the results.

There were some differences in the I_{SC} values in the initial measurement (Table 1). To investigate the difference a bit further, IPCE measurements were carried out. Those measurements indicated that firstly absolute maximum quantum efficiency ($IPCE_{MAX}$) was higher in the nanocellulose cells compared to the reference cells (Figure 4a) as was to be expected based on the photovoltaic measurements. The normalized IPCE spectra in Figure 4b shows that there is a systematic red shift in the IPCE data in the nanocellulose cells compared to the reference cells in the wavelengths higher than 520 nm. This means that the nanocellulose cells were utilizing the long wavelengths more efficiently than the reference cells.

The results, i.e. the increased $IPCE_{MAX}$ (Figure 4a) and red shift of the spectra (Figure 4b) in the nanocellulose cells, are very similar to the literature results when differences caused by electrolyte filling have been detected and they are specifically typical for the case where there is a reduced amount of voltage increasing agents (4-tBP and NMBI) [4,20]. Firstly, the absolute increase in $IPCE_{MAX}$ in the nanocellulose cells could be linked with the increased electron injection as discussed in the previous section. Secondly, the red shift has been hypothesized to

be related with the thiocyanate ligand exchange [4,21,22]. The individual cell that was prepared and filled with electrolyte similar to the nanocellulose cells but without the nanocellulose, that was discussed in previous section, had similar IPCE spectra as the nanocellulose cells and for instance the normalized IPCE spectra had a perfect match. These factors further support our hypothesis that the electrolyte filling method in the nanocellulose cells is mainly causing the differences in the nanocellulose cells rather than the nanocellulose itself.

3.4 The effect of the nanocellulose layer to charge transfer in the cell

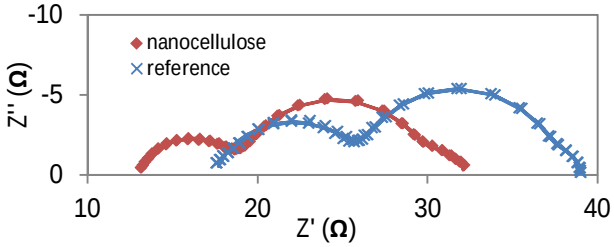

Figure 5. Examples of the EIS spectra measured at open circuit conditions under 1 Sun illumination. The measured data is indicated with the markers and the equivalent circuit fits with the solid lines.

Table 2. Average resistances and related standard deviations in the initial EIS measurements done under 1 Sun illumination.

	number of cells	R_S [Ω]	R_{CE} [Ω]	Z_d [Ω]
nanocellulose cells	3	15 ± 3	6.4 ± 1.8	3.4 ± 1.9
reference cells	4	18 ± 2	8.6 ± 2.6	2.0 ± 0.4

The EIS measurements at open circuit are suitable for quantitative comparison of the internal resistances with the exception of the resistance of photoelectrode / electrolyte interface R_{PE} [19]. This is because the current and hence also voltage over the other interfaces are zero in case of all the other components than photoelectrode/electrolyte which is polarized to V_{OC} which varies from cell to cell. In this section we discuss the difference resistance in the cell expect for R_{PE} which is examined using dark EIS measurement in Section 3.5. Examples of the measured and fitted data are shown in Figure 5. The equivalent circuits used here are presented in our previous work [17]. The EIS data in Table 2 showing all the measured data indicates that there were only small differences in the average resistances between the nanocellulose and reference cells. When taking into account the cell to cell variation described by the standard deviation, there are no significant differences between the cells. The cell to cell variations arise most likely from the fact that handwork is needed in the preparation of the cells. For instance the exact placement of the copper contact and the silver paint can easily result in small differences in sheet resistance R_S as shown in Table 2. Interestingly, the charge transfer resistance between the counter electrode catalyst and the electrolyte, R_{CE}, is not any larger in the nanocellulose cells compared to the reference cells (Table 2). This indicates that the

nanocellulose layer did not significantly block the counter electrode catalyst / electrolyte interface. The presence of nanocellulose could also affect the diffusion of the charge transfer in the electrolyte as there is some reduction in the volume of the free electrolyte and it creates some tortuosity. However, the charge transfer of the electrolyte at the counter electrode Z_d was not greatly influenced either (Table 2). As the nanocellulose was highly porous (Section 3.1) and the structure of the aerogel membrane relatively open, as suggested by the SEM studies, the used membrane did not seem to hinder the diffusion significantly. Hence the deduction that was made based on the R_{cell} value (Table 1) in Section 3.2 is repeated when its individual components (R_S, R_{CE} and Z_d) are examined.

3.5 Charge transfer at the photoelectrode

Here we see a decrease in the charge transfer resistance at the photoelectrode / electrolyte interface R_{PE} in the nanocellulose cells compared to the reference cells. Our hypothesis states that in the reference cells there would be more voltage increasing agent in the dyed TiO_2 films. In the literature such an increase has correlated with decreased rate of recombination (higher R_{PE}) [17] which is exactly what is seen also here (Figure 6a). In terms of capacitance at the photoelectrode / electrolyte interface C_{PE}, the nanocellulose cells have higher value than the reference cells (Figure 6b). More precisely there appears to be about 100 mV shift in the voltage (Figure 6b) which is the same order as the shift in V_{OC} in the photovoltaic measurements (60 ± 20 mV; Table 1). The nanocellulose cells had also a bit higher I_{SC} (Table 1) and a higher current would increase also V_{OC} slightly which bridges the gap between V_{OC} values of the reference and nanocellulose cells even more. These pieces of data imply that the conduction band has shifted as suggested in Section 3.2 and 3.3 and that would cause the majority of differences between the cells. The effective electron lifetime τ can be calculated as a product of R_{PE} and C_{PE} [23-26]. At voltage range 0.4-0.7 V, the nanocellulose and the reference cells do not have any clear difference between them (Figure 6c). Neither our previous studies have showed any significant differences in τ when there were apparent differences in the amount of voltage increasing agents [5]. As in the previous Sections, also here the individual cell without nanocellulose but filled similar to the nanocellulose cells was giving the same kind of EIS response as the nanocellulose cells which again implies that also the differences seen here are caused by changes in the filling method and not by the nanocellulose itself.

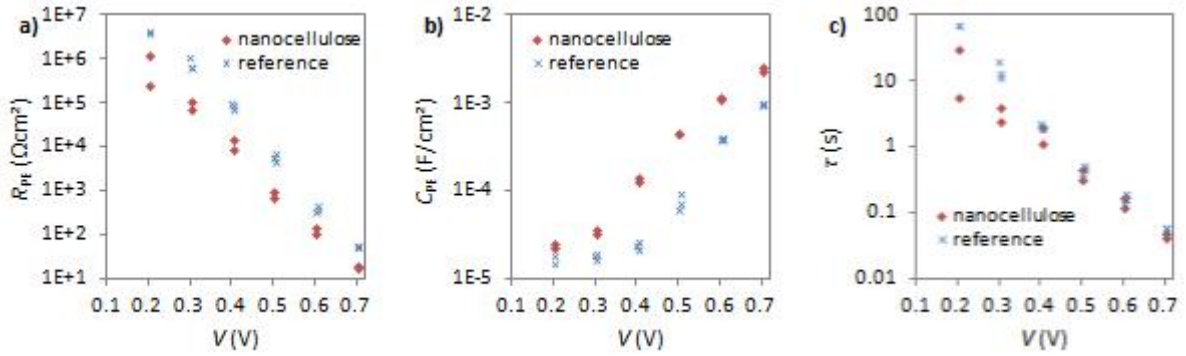

Figure 6. EIS data describing the photoelectrode performance in the initial measurements: a) R_{PE}, b) C_{PE} and c) τ. Data from 2-3 similar type of cells are plotted to illustrate the repeatability.

3.6 Stability of the cells

A critical issue when adding this kind of a membrane in the cell is that it does not react with the other components in the cell and the stability of the device remains high. Here the cells were aged for 1000 h in 1 Sun equivalent at 40 ºC. The nanocellulose cells were as stable as the reference cells. All the tested cells retained about 90 % or more of their initial efficiency after the aging test based on the solar simulator measurements. An example of the recorded aging data of a nanocellulose cell is shown in Figure 7. In Figure 7 the values in aging data differ slightly from the values that have been measured with the solar simulator because of differences in measurement setups (explained in Section 2). Based on this aging testing and solar simulator results it can be concluded the nanocellulose membrane does not appear to affect the lifetime of the cells.

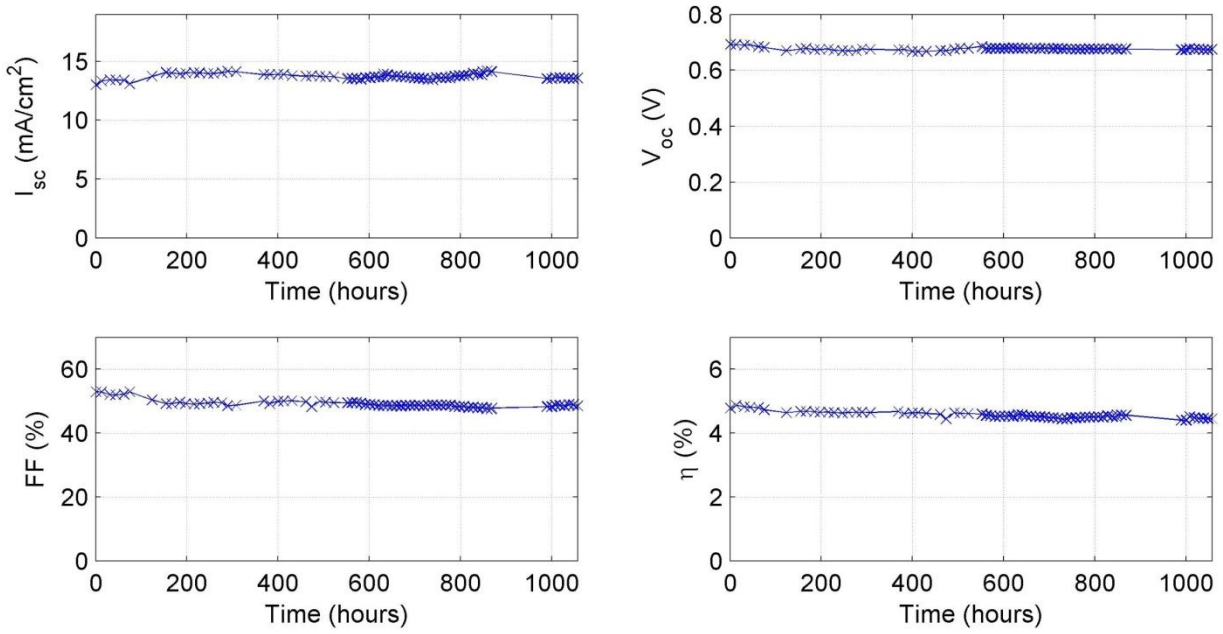

Figure 7. An example aging data of a nanocellulose cell under approximately 1 Sun illumination at 40 ºC.

4. Conclusions

A new method for filling the dye-sensitized solar cells with an electrolyte using a highly porous nanocellulose aerogel membrane was introduced in a proof-of-concept manner. Freeze-drying a screen printed nanocellulose hydrogel film allowed deposition of the organic liquid electrolyte in a way that intrinsically lead to an even electrolyte distribution as the electrolyte did not flow

through the cell but was added as droplet to the aerogel film that acted as a sponge. Another clear technological advantage was that no electrolyte filling holes were needed in the preparation of these cells which simplifies the sealing of the cells greatly as well as eliminates one pathway for leakage.

The addition of the nanocellulose aerogel as a solid support for the liquid electrolyte did not affect the efficiency of the DSCs compared to conventional reference cells with liquid electrolyte, which is the goal when semi-solid electrolytes are investigated. The analysis of the charge transfer processes revealed that the nanocellulose did not increase the charge transfer resistance at the counter electrode / electrolyte interface nor the diffusion of the electrolyte compared to the reference devices. It can be concluded that the printed nanocellulose layer did neither block the catalyst reaction nor complicate the diffusion in the electrolyte significantly. Furthermore, the stability analysis confirmed that the cells with nanocellulose were as stable as the reference cells. Hence the nanocellulose membrane appeared to be inert when considering the performance and the stability of the cells.

Acknowledgements

We thank VTT Technical Research Center of Finland and UPM for the preparation of the nanocellulose hydrogel. K.M. is grateful for post doctoral project (253643) funded by the Academy of Finland, and J.V. for post doctoral grant funded by Emil Aaltonen foundation. This work was partially funded also by Academy Finland (project SOLID, 271081) and Multidisciplinary Institute of Digitalization and Energy (MIDE) of Aalto University (project FerroPV; 751026). This work made use of the Aalto University Nanomicroscopy Center (Aalto-NMC) premises and we thank Dr. Juuso Korhonen for taking the SEM images and useful discussions.

References

[1] J. Kalowekamo, E. Baker, Solar Energy 83 (2009) 1224-1231.
[2] G. Hashmi, K. Miettunen, T. Peltola, J. Halme, I Asghar, K. Aitola, M. Toivola, P. Lund, Renewable and Sustainable Energy Reviews 15 (2011) 3717-3732.
[3] K. Miettunen, J. Halme, P. Lund, Electrochemistry Communications, 11 (2009) 25-27.
[4] K. Miettunen, M.I. Asghar, S. Mastroianni, J. Halme, P.R.F. Barnes, E. Rikkinen, B.C. O'Regan, P. Lund, Journal of Electroanalytical Chemistry 664 (2012) 63-72.
[5] K. Miettunen, P.R.F. Barnes, X. Li, C.H. Law, B.C. O'Regan, Journal of Electroanalytical Chemistry 677-680 (2012) 41-49.
[6] S.G. Hashmi, K. Miettunen, A. Ruuskanen, M.I. Asghar, J. Halme, P. Lund, Proceedings of the 27th European Photovoltaic Solar Energy Conference 27 (2012) 2922-2924.
[7] A. Priya, A. Subramania, Y. Jung, K. Kim, Langmuir, 24 (2008) 9816-9819.
[8] S. J. Lue, P. W. Lo, L.-Y. Hung, Y. L. Tung, Journal of Power Sources, 195 (2010) 7677-7683.
[9] J. T. Korhonen, M. Kettunen, R. H. A. Ras, O. Ikkala, ACS Applied Materials & Interfaces 3 (2011) 1813-1816.
[10] T. Saito, Y. Nishiyama, J. Putaux, M. Vignon, A. Isogai, Biomacromolecules 7 (2006), 1687-

1691.
[11] T. Saito, S. Kimura, Y. Nishiyama, A. Isogai, Biomacromolecules 8 (2007) 2485-2491.
[12] M. Paakko, J. Vapaavuori, R. Silvennoinen, H. Kosonen, M. Ankerfors, T. Lindström, L. A. Berglund, O. Ikkala, Soft Matter 4 (2008) 2492-2499.
[13] S. Ito, P. Liska, P. Comte, R. Charvet, P. Péchy, U. Bach, L. Schmidt-Mende, S. Zakeeruddin, Chemistry Communications 14 (2005) 4351-4353.
[14] S. Ito, K. Nazeeruddin, P. Liska, P. Comte, R. Charvet, P. Péchy, M. Jirousek, A. Kay, S. Zakeeruddin, M. Grätzel, Progress in Photovoltaics: Research and Applications, 14 (2006) 589-601.
[15] J.T. Korhonen, P. Hiekkataipale, J. Malm, M. Karppinen, O. Ikkala, R. Ras, ACS Nano 5 (2011) 1967-1974.
[16] Md.K. Nazeeruddin, A. Kay, I. Rodicio, R. Humphry-Baker, E. Müller, P. Liska, N. Vlachopoulos, M. Grätzel, Journal of American Chemical Society 115 (1993) 6382-6390.
[17] S.A. Haque, E. Palomares, B.M. Cho, A.N.M. Green, N. Hirata, D.R. Klug, J.R. Durrant, J. Am. Chem. Soc., 127 (2005) 3456-3462.
[18] G. Schlichthörl, S.Y. Huang, J. Sprague, A.J. Frank, Journal of Physical Chemistry B 101 (1997) 8141-8155.
[19] J. Halme, P. Vahermaa, K. Miettunen, P. Lund, Advanced Materials 22 (2010) E210-E234.
[20] G. Boschloo, H. Lindström, E. Magnusson, A. Holmberg, A. Hagfeldt, J. Photochem. Photobio. A: Chem. 148 (2002) 11-15.
[21] Md.K. Nazeeruddin, P. Péchy, M. Grätzel, Chemical Communications 18 (1997) 1705-1706.
[22] Md.K. Nazeeruddin, P. Péchy, T. Renouard, S.M. Zakeeruddin, R. Humphry-Baker, P. Comte, P. Liska, L. Cevey, E. Costa, V. Shklover, L. Spiccia, G.B. Deacon, C.A. Bignozzi, M. Grätzel, Journal of American Chemistry Society 123 (2001) 1613–1624.
[23] J. Bisquert, Physical Chemistry Chemical Physics, 5 (2003) 5360-5364.
[24] A. Pitarch, G. Garcia-Belmonte, I. Mora-Sero, J. Bisquert, Physical Chemistry Chemical Physics 6 (2004) 2983-2988.
[25] J. Bisquert, Journal of Physical Chemistry B 108 (2004) 2323-2332.
[26] J. Bisquert, F. Fabregat-Santiago, I. Mora-Sero, G. Garcia-Belmonte, S. Gimenez, Journal of Physical Chemistry C 113 (2009) 17278-17290.